JOURNAL OF MATERIALS SCIENCE 20 (1985) 438–448

Plastic deformation of glassy amorphous polymers: influence of strain rate

J. M. LEFEBVRE, B. ESCAIG
Laboratoire de Structures et Propriétés de l'Etat Solide CNRS (LA 234), Université des Sciences et Techniques de Lille, 59655 Villeneuve d'Ascq Cedex, France

The compressive deformation of glassy atactic polymethyl methacrylate has been studied in the temperature range $150 < T < 330$ K as a function of applied strain rate. Special emphasis is given to the definition of an elementary activation rate, i.e. the characteristic frequency of the successful plastic deformation events. This determines the frequency at which the elastic counteraction of the medium to the nucleation of plasticity has to be taken into account, in order to ensure self-consistence of the kinetic and thermodynamic analysis of deformation previously proposed.

1. Introduction

The yielding phenomenon of glassy polymers generally results in the formation of localized shear bands, the degree of heterogeneity of which being strongly dependent on the past thermomechanical treatments the samples have undergone.

Though a distinction was formerly established between shear bands and diffuse zones [1], more precise structural observations revealed in both cases the existence of well-defined bands, either coarse or fine [2]. These bands originate from the nucleation and growth of shear nuclei past a critical size. The present approach describes the stress-aided thermally activated growth of these nuclei and the overcoming of energy barriers responsible for yielding. The thermodynamic and kinetic analysis developed [3] is aimed at establishing the characteristic features of the elementary mechanism, namely its energy and spatial extension. This requires a precise definition of concepts and activation parameters together with a careful examination of the corresponding experimental operational quantities. When expressing the stress and temperature dependence of the strain rate in the form of a simple Arrhenius law:

$$\dot{\epsilon} = \dot{\epsilon}_0 \exp - \frac{\Delta G_a(\sigma, T)}{kT} \quad (1)$$

it is of great importance to make a clear distinction between the free energy ΔG_a and the activation enthalpy ΔH_a, which means that the activation entropy ΔS_a has also to be dealt with. This last term mainly originates from the temperature dependence of the energy barrier through that of the elastic constants $\mu(T)$ in the temperature range investigated. Illustrations of the procedure have been given in the case of polystyrene (PS) and polymethyl methacrylate (PMMA) at a particular strain rate [4, 5]. The results established the existence of two different deformation modes on either side of a critical temperature, T_c. Since then, new implications of the theory have been introduced in the refinement of data treatment [6, 7] and it is the purpose of this paper to apply it to the influence of strain rate on the plastic deformation behaviour of PMMA.

In a first section the essentials of the thermodynamic analysis are briefly recalled, the operational parameters defined and their informational content checked in a self-consistent way. The next part details the experimental procedures and results. The deformation scheme obtained is discussed in the last section and data from the literature are incorporated which result in a quite reasonable agreement.

2. Thermal activation analysis

2.1. Thermodynamic analysis

Owing to the relatively large relaxation times of structural variations in the glassy state ($\tau_R \gtrsim 10^2$ sec), the stress-aided thermally activated growth of shear nuclei can be treated by standard quasi-equilibrium thermodynamics since characteristic time for the elementary deformation events τ_{def} are in the range 10^{-3} to 10^{-5} sec (see Section 2.2 below).

We define as a state variable the entropic strain ϵ_s produced by uncoiling bonds within the shear nucleus, which is proportional to the nucleus size V. The polymer sample being considered in its whole, the sample average strain is thus defined as $\epsilon_s = (V/V_{\text{tot}})\Delta e_0$ where V_{tot} is the sample volume and Δe_0 is the elementary shear in the nucleus, a monomer cage parameter of order unity [8]. (Note that V might be used as well as a reaction variable.) Developments of the calculation (see [3, 6, 7]) lead to an estimate of the free energy variation of the system (sample plus external sources of stress) during a reversible and isothermal variation $d\epsilon_s$ under constant pressure, temperature and applied stress σ_a conditions.

We can thus define the Gibbs free energy of activation ΔG_a as the integral over the barrier of the variation of the thermodynamic potential of the system, and as the most important result, explicitly its partial derivatives at constant pressure and structure, namely the entropy of activation $\Delta S_a = -(\partial \Delta G_a/\partial T)_{P,\sigma_a,\text{struct.}}$ and the activation volume $V_a = -(\partial \Delta G_a/\partial \sigma_a)_{P,T,\text{struct.}}$.

V_a is directly related to the critical size of the shear nucleus V_c and it reflects the spatial extent of the zone where monomer units undergo coherent thermal fluctuations.

ΔS_a is related to the temperature dependence of the elastic counteraction of the material to the growth of the nucleus. Assuming the corresponding energy to be proportional to the shear modulus $\mu(T)$ leads to an entropy increase due to the change of the vibrational spectra of molecules with temperature. Apart from the usual softening of spring-like intermolecular forces as temperature rises, a specific contribution to $d\mu/dT$ in the case of polymeric materials comes from the drop of the shear modulus in the temperature range corresponding to the secondary mechanical relaxations (T_β, T_γ, . . .), i.e. to the onset of local molecular movements on the chain. The resulting entropy term is much larger than that usually encountered in crystalline materials.

At last the preponderance of these Hookean contributions is established, as compared to rubber-like terms originating from bond uncoiling [1, 6, 7]. Using these assumptions, the Gibbs free energy of activation is expressed in the following way [1, 6, 7].

$$\Delta G_a = (\Delta H_a + x\sigma_a V_a)(1-x)^{-1} \tag{2}$$

where

$$x = T/\mu \times d\mu/dT.$$

ΔG_a can also be deduced in a different manner by integrating its stress derivative V_a: this implies building from $\Delta G_a(\sigma_a, T)$ a single variable function which is independent of temperature. This is achieved by scaling ΔG_a by the shear modulus and we finally obtain:

$$\Delta G_a = \frac{\mu}{\mu_0} \int_{\tau_a}^{\tau_a(0)} V_a(\tau_a)\, d\tau_a \tag{3}$$

with the reduced variable $\tau_a = (\mu_0/\mu)\sigma_a$ [3, 9] where $\tau_a(0)$ and μ_0 refer to zero K.

As far as suitable experimental information is available we are thus able to characterize the elementary deformation mechanism by its specific free energy of activation ΔG_a and by its spatial extent V_a.

2.2. Deformation kinetics

The macroscopic strain rate resulting from the expansion of shear nuclei past their critical configuration may be expressed from the general formulation of activated flow as:

$$\dot{\epsilon} = N\epsilon_0 R \tag{4}$$

where N is the number of active sites and ϵ_0 the average deformation resulting from each successful event.

The activation rate R characterizes the fraction of those nuclei that achieves expansion per unit time. R is the product of a frequency factor and a Boltzmann factor [10]:

$$R = \nu_N \exp - \left[\frac{\Delta G_a(\sigma, T)}{kT}\right],$$

the second right-hand term expressing the probability at equilibrium of a fluctuation in energy greater than ΔG_a.

Equations 1 and 4 thus give

$$\dot{\epsilon} = N\epsilon_0\nu_N \exp - \left[\frac{\Delta G_a(\sigma, T)}{kT}\right]$$

or

$$\Delta G_a = kT \ln\left(\frac{N\epsilon_0\nu_N}{\dot{\epsilon}}\right) = \alpha kT$$

which means that when a single mechanism is rate-controlling ΔG_a is directly proportional to temperature under constant strain rate conditions.

The activation rate R can be viewed as the characteristic frequency of the nucleation process, $\nu_{\text{def}} = R$, or its inverse, $\tau_{\text{def}} = R^{-1}$, as the characteristic time of the elementary event for plastic deformation. In a constant strain rate test, this time is a constant, and can be written as:

$$\tau_{\text{def}} = \nu_N^{-1} \exp \alpha = N\epsilon_0 \dot{\epsilon}^{-1} \qquad (5)$$

For a typical value $\alpha \simeq 20$, and $\nu_N \simeq 10^{12}\,\text{sec}^{-1}$ [3, 6, 7], $\tau_{\text{def}} \simeq 5 \times 10^{-4}$ sec, which justifies the quasi-equilibrium treatment given in Section 2.1. The evaluation of this time turns out to be an essential step in the present analysis.

A major aim of the analysis is to yield the Gibbs free energy characteristic of the process, i.e. ΔG_a. As recalled in Section 2.1, this determination either from Equation 2 or from Equation 3 requires independent knowledge of the temperature dependence of the elastic constants in the form of the data $(\mathrm{d} \ln \mu/\mathrm{d}T)$. Hence the question arises of deciding first at which frequency ν_{mod} the elastic response of the material should be taken.

In previous attempts in the literature to describe the yield behaviour of glassy polymers, either by nucleating disc-shaped shear zones [8], or by kinking a bundle of molecular rods [11], the elastic response of the medium was simply taken at a frequency of 1 Hz for the ease of available experimental data and without further justification. We think this treatment is not grounded, and invalidate partly the experimental check of theoretical models.

An alternative analysis of yielding by modified Ree–Eyring formulation correlated the yield stress behaviour to the dissipative component of the dynamic modulus through an *ad hoc* rheological spring-and-dashpot analogue [12, 13]. Following this parameter fitting analysis, a "knee" can be defined on the curve of yield stress against temperature above which temperature alone is enough to activate the β-processes involved in deformation (assumed to be in parallel with α-processes), that is to say above which β barriers become "transparent" to thermal activation and do not require any further aid of stress. Therefore the frequency of a "corresponding" dynamical test can be defined as that at which the β-peak temperature is identical to the knee temperature on the yield stress–temperature curve. Application to polycarbonate thus yields a characteristic frequency $\nu_{\text{mod}} \simeq 2.3 \times 10^3 \dot{\epsilon}$, as deduced from the deformation (and dynamical) parameters proposed by parameter fitting for this polymer. However, the above procedure relies entirely on the *ad hoc* rheological analogue introduced from the beginning in the analysis on the basis of six fitting parameters without real physical meaning (e.g. very high values of frequency factors, activation volumes *a priori* stress independent, see [5] for discussion). Therefore the presented correlation appears to be somewhat artificial, and a more physically grounded determination is needed for the frequency ν_{mod}.

The basic question of choosing the relevant frequency capable of describing correctly the elastic constants of the medium during the defect nucleation process, is not an obvious one. Let us put the physical problem in the following way. Suppose we watch over a given time the whole assembly of active shear nuclei trying to achieve growth just as coherent thermal fluctuations of chain segments create them at a time with a certain size, and destroy them out the time after (when too small) with a trial frequency ν_N close to the Debye frequency ($\nu_N \simeq 0.1 \nu_D$ [3].) As a first guess, one might think that the effective shear modulus to use in the opposing energy barrier should be that experienced during one trial, i.e. the shear modulus at frequency ν_N. However, most of these trials do not succeed – only one in a time $\tau_{\text{def}} = R^{-1}$ does. During that time, any local movement of molecular segments of the δ, γ or β type as well, either in-chain or sideways but fast enough to occur between two successful events, will contribute a relaxed shear modulus to energy barriers. It is clear that the succeeding nuclei will be most likely to be located where barriers are thus lowered so that the shear modulus experienced by *successful* nuclei should be the same as that which would be measured at a frequency:

$$\nu_{\text{mod}} = \nu_{\text{def}} = R = (N\epsilon_0)^{-1} \dot{\epsilon} \qquad (6)$$

A practical problem arises then, since ν_{def} is not known *a priori*, and requires the introduction of ν_{mod} in order to be determined from thermodynamical analysis. An iterative procedure has therefore to be used until reasonable consistency is achieved, i.e. until the ratio $\nu_{\text{def}}/\nu_{\text{mod}}$ is much less than one decade. It can be represented schematically as follows:

$$\frac{d\mu}{dT}(\nu_{\mathrm{mod}\,1}) \rightarrow \Delta G_{a_1} = \alpha_1 kT \rightarrow \nu_{\mathrm{def}\,1} \equiv \nu_{\mathrm{mod}\,2}$$

$$\rightarrow \frac{d\mu}{dT}(\nu_{\mathrm{mod}\,2}) \rightarrow \Delta G_{a_2} = \alpha_2 kT$$

$$\rightarrow \nu_{\mathrm{def}\,2} \equiv \nu_{\mathrm{mod}\,3} \rightarrow \ldots$$

In practice, as illustrated below, the obtaining of an optimized frequency is achieved in two or three steps.

2.3. Operational parameters

The usual method is to derive operational apparent quantities relating strain rate, applied stress and temperature at comparable structural states. On this last point a proper definition of the yield stress has been given elsewhere [4, 5].

Our interest concentrates on two parameters: the temperature sensitivity of the strain rate; and the stress sensitivity of the strain rate. These are generally defined in the following way [3]:

$$\Delta H_0 = kT^2 \left(\frac{\partial \ln \dot{\epsilon}}{\partial T}\right)_{\sigma_a, \mathrm{struct.}}$$

$$V_0 = kT \left(\frac{\partial \ln \dot{\epsilon}}{\partial \sigma_a}\right)_{T, \mathrm{struct.}}$$

Introducing these expressions into Equation 1 one obtains:

$$\Delta H_0 = kT^2 \left(\frac{\partial \ln \dot{\epsilon}_0}{\partial T}\right)_{\sigma_a, \mathrm{struct.}} + \Delta G_a + T\Delta S_a$$

$$V_0 = kT \left(\frac{\partial \ln \dot{\epsilon}_0}{\partial \sigma_a}\right)_{T, \mathrm{struct.}} + V_a$$

$\dot{\epsilon}_0$ reflects the stress and temperature dependence of structure terms (density of active sites, size of nuclei); $\dot{\epsilon}_0$ is generally weakly temperature dependent, and if so remains negligible by comparison to the exponential term in Equation 1.

This means that a determination of ΔH_0 at constant structure provides a reliable measure of the activation enthalpy: $\Delta H_0 \simeq \Delta H_a$. The stress dependence of $\dot{\epsilon}_0$ is often described in the form of a power law $\dot{\epsilon}_0 \sim (\sigma_a - \sigma_i)^n$ with $n \lesssim 4$ (for n values much higher, it is more reasonable to express the stress dependence in the exponential term). The structural parameter σ_i depicts the arrangement of defects, i.e. the past thermomechanical history.

The operational activation volume can thus be written:

$$V_0 = \frac{nkT}{\sigma_a - \sigma_i} + V_a$$

and the first term on the right-hand side may be important, especially at high temperature when the effective stress $\sigma_a - \sigma_i$ is small.

V_0 is deduced from a stress relaxation test (see e.g. [5, 14]) and ΔH_0 either from a temperature jump at constant strain rate or from the expression $\Delta H_0 = -TV_0(\partial \sigma_a/\partial T)_{\dot{\epsilon}, \mathrm{struct.}}$ by a combination of the operational activation volume and the slope of the curve of yield stress against temperature.

We may sum up as follows:

(1) The determination of ΔG_a from Equation 2 brings the first indication of a single rate-controlling mechanism. In such a case the plot of ΔG_a against T is a straight line going through the origin.

(2) The integration method of Equation 3 agrees with the above determination as long as the operational quantity V_0 has the physical meaning of an activation volume, i.e. $V_0 \simeq V_a$. The disagreement between the two routes indicates the critical temperature beyond which the stress dependence in the pre-exponential term is no more negligible.

(3) The determination of the characteristic deformation frequency ensures a self-consistent evaluation of the entropy term and of ΔG_a.

(4) No adjustable parameter is involved in the present analysis.

3. Experimental details and results

3.1. Experimental procedure

The PMMA used in this study was prepared by anionic polymerization at the Ecole d'Application des Hauts Polymères, Strasbourg. Its molecular weight distribution, as deduced from GPC measurements is characterized by $\bar{M}_{\omega} = 223\,000$ and a polydispersity $p = 2.29$. Its glass transition temperature is $T_g = 380\,\mathrm{K}$. Details of the compression moulding and annealing procedures have been given elsewhere [5]. The resulting material may thus be considered as well-annealed, with little ageing effects within the time allowed before deformation.

Cylindrical samples were compression tested in an Instron machine in the temperature range $150 < T < 330\,\mathrm{K}$ at constant applied strain rate $10^{-5}\,\mathrm{sec}^{-1} < \dot{\epsilon} < 10^{-3}\,\mathrm{sec}^{-1}$. Elastic modulus measurements were performed for frequencies varying from 1 to $10^3\,\mathrm{Hz}$. The 1 Hz data were obtained on a torsion pendulum at the ENSMA, Poitiers and data ranging from 7.8 to $10^3\,\mathrm{Hz}$ on

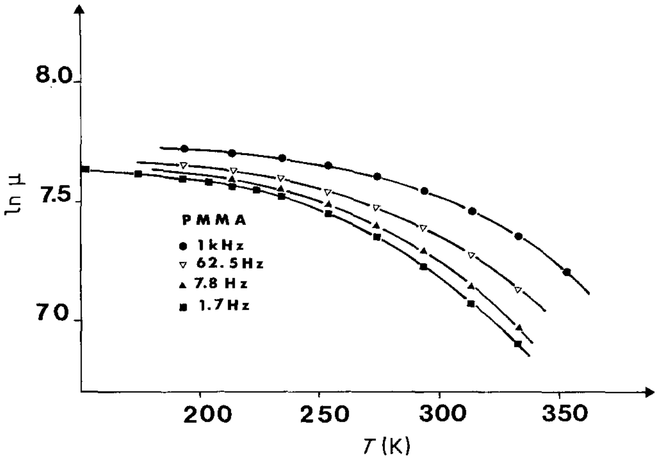

Figure 1 Variation of the shear modulus with temperature (logarithmic scale, μ in MPa).

the viscoelasticimeter – Metravib. The results are summarized in Fig. 1 in the form $\ln \mu$ against T, since the quantity of interest is $(1/\mu) \times (\mathrm{d}\mu/\mathrm{d}T)$.

3.2. Results

The variation of yield stress with temperature for three different strain rates is shown in Fig. 2. The lowest strain rate $\dot{\epsilon} = 3.5 \times 10^{-5}\,\mathrm{sec}^{-1}$ was used in the analysis previously published [5]. To avoid repetition, we merely recall here that it was shown in [5] that there was good agreement between determinations of ΔG_a by the two routes mentioned above, below $T_\mathrm{c} \simeq 200\,\mathrm{K}$, with the result $\Delta G_\mathrm{a} \simeq 18\,kT$. The elastic modulus was taken at that time as usual, i.e. in the one cycle range, but it was already concluded that a consistent analysis would involve measuring $\mu(T)$ in the kilocycle range since $R = \nu_\mathrm{def} = \nu_\mathrm{N} \exp - \alpha \simeq 10^4\,\mathrm{sec}^{-1}$.

These data have thus been reconsidered using the more suitable measurements shown in Fig. 1. Using the shear modulus $\mu(T)$ observed at 10^3 Hz gives finally the result illustrated in Fig. 3 where the Gibbs free energy of activation exhibits two distinct behaviours in the temperature range

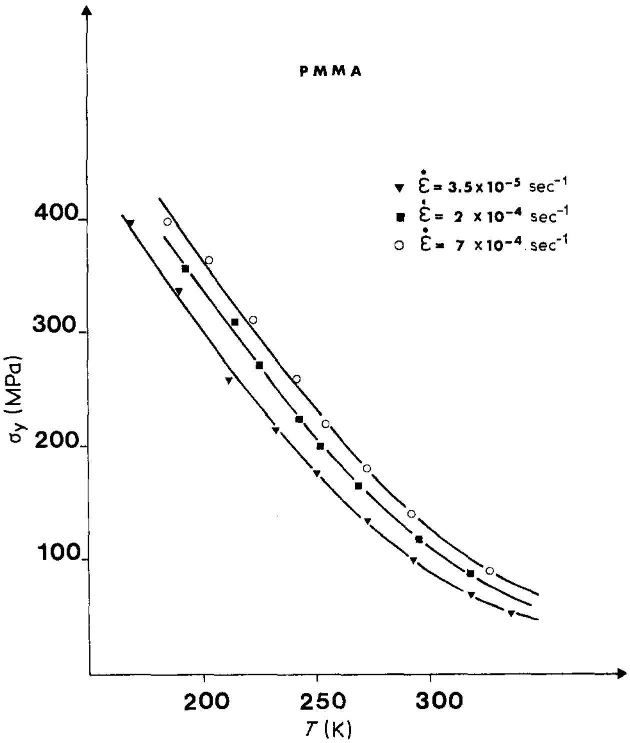

Figure 2 Variation of the yield stress with temperature at three different strain rates.

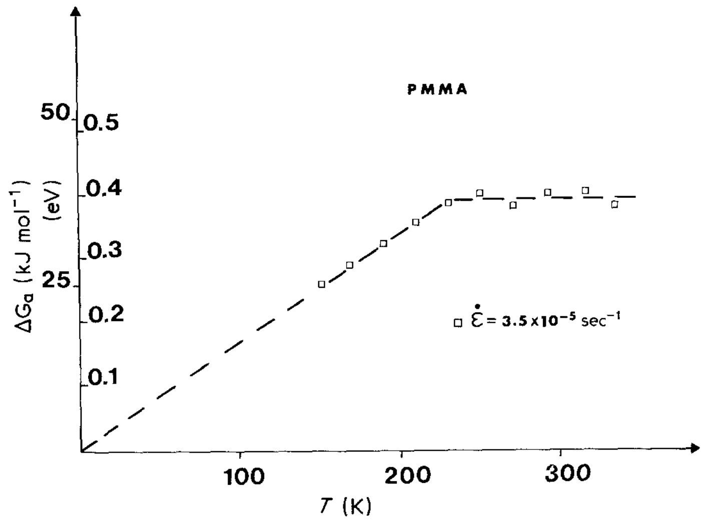

Figure 3 Variation of the Gibbs free energy of activation with temperature ($\dot{\epsilon} = 3.5 \times 10^{-5}$ sec^{-1}).

investigated:

$$T < T_c \simeq 230 \pm 10\,\text{K};\ \Delta G_a = \alpha kT \quad \alpha \simeq 20$$

$$T > T_c;\ \Delta G_a = \Delta G_m = 0.39 \pm 0.03\,\text{eV}$$

$$(\simeq 38\,\text{kJ mol}^{-1})$$

This plot gives a value $\nu_{\text{def}} \simeq 2 \times 10^3$ Hz, in good agreement with the initial value for ν_{mod}, $\nu_{\text{mod}} = 10^3$ Hz.

For the sake of clarity, we illustrate now the procedures explained in Section 2 in the case of the highest strain rate, $\dot{\epsilon} = 7 \times 10^{-4}$ sec^{-1}. From the temperature variation of yield stress in Fig. 2 and that of operational activation volume in Fig. 4 we deduce the values of Table I with the elastic term $(1/\mu) \times (\mathrm{d}\mu/\mathrm{d}T)$ taken at 10^3 Hz. In a first step (not reproduced here, see e.g. [4, 5]) calculation of ΔG_a from Equations 2 and 3 has established that the operational parameter V_0 is equal to the true activation volume V_a for $T_c \lesssim 250$ K. Accordingly, subsequent calculation leading to ΔG_{a_1} in Table I introduces $V_a = V_0$ for $T < 250$ K and the extrapolation along the dotted line on Fig. 4 for $T > 250$ K. Both ΔG_{a_1} and ΔG_{a_2} are obtained from Equation 2.

TABLE I Activation parameters for $\nu_{\text{mod}} = 10^3$ Hz. For PMMA $\dot{\epsilon}_p = 7 \times 10^{-4}$ sec^{-1}

T (K)	σ_a (MPa)	ΔH_0 (kJ mol^{-1})	ΔG_{a_1} (kJ mol^{-1})
185	396	30.8	25
204	360	33.7	27
223	310	40.5	28.9
242	258	53	32.7
254	218	60.7	33.7
273	176	65.5	30.8
292	138	77	32.8
326	90	92.5	27

The variation of ΔG_{a_1} with temperature is shown in Fig. 5. Its low temperature part yields $\Delta G_{a_1} \simeq 16kT$, and at high temperatures ΔG_{m_1} sensibly differs from the value obtained at $\dot{\epsilon} = 3.5 \times 10^{-5}$ sec^{-1}. However, it seems rather doubtful from the increase of T_c with $\dot{\epsilon}$, and Equation 1, that $\dot{\epsilon}$ might also affect ΔG_m. In fact one has to consider again the elementary activation frequency: $\nu_{\text{def}} = \nu_N \exp - 16 \simeq 100$ kHz, so that $\nu_{\text{def}}/\nu_{\text{mes}} \sim 100$. The lack of experimental methods available in our laboratory in the range 10^3 to 10^6 Hz is fortunately solved by a recent work of Read [15].

Fig. 6 reproduces the variation of the logarithm of the shear modulus with temperature deduced from his data for different frequencies between 1 and 10^6 Hz. Though imprecise, this plot permits us to estimate the temperature shift needed to superimpose the different curves. Comparing data at 7.8 and 10^3 Hz, gives a corresponding shift of 35 ± 2 K from our own measurements (Fig. 1), against 37 ± 2 K from Read's measurements (Fig. 6). This good agreement gives us confidence in using Fig. 6 to estimate the shifts ΔT valid for frequencies higher than 10^3 Hz and apply them to our data at 10^3 Hz, so as to obtain data for frequencies $\nu_2 > 10^3$ Hz:

$$\frac{1}{\mu}\frac{\mathrm{d}\mu}{\mathrm{d}T}(T_1, \nu_1 = 10^3\,\text{Hz}) = \frac{1}{\mu}\frac{\mathrm{d}\mu}{\mathrm{d}T}(T_1 + \Delta T, \nu_2).$$

The ΔG_{a_2} values of Fig. 5 are thus calculated with a modulus variation evaluated at 10^4 Hz

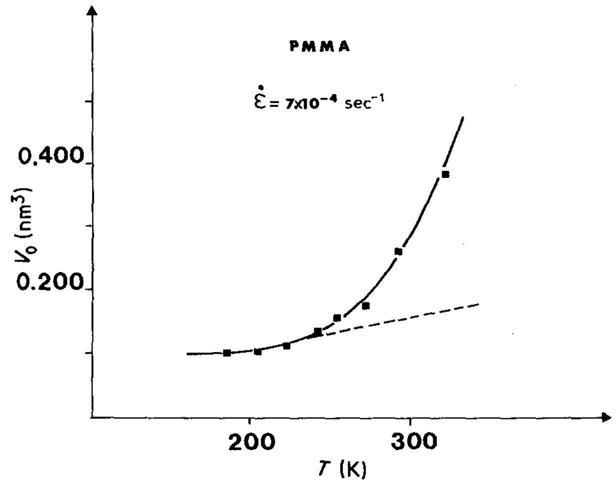

Figure 4 Variation of the operational activation volume with temperature ($\dot{\epsilon} = 7 \times 10^{-4}$ sec^{-1}).

through a shift $\Delta T \simeq 17$ K. These lead to $T_c \simeq 255 \pm 10$ K and $\Delta G_{a_2} \simeq 18\,kT$, which in turn yield $\nu_{\text{def}} \simeq 1.3$ to 1.5×10^4 Hz, in good agreement with $\nu_{\text{mod}} = 10^4$ Hz.

As a last result, ΔG_m is found independent of $\dot{\epsilon}$:

$$\Delta G_m = 0.39 \pm 0.03 \text{ eV}.$$

Though data treatment may seem rather tedious, note that there is no parameter-fitting in it, and it is merely aimed at self-consistence of both thermodynamic quantities and experimental operational parameters.

Experimental results for $\dot{\epsilon} = 2 \times 10^{-4}$ sec^{-1} are treated in the same way, with the same kind of ΔG_a against T diagram, i.e.: ΔG_a proportional to temperature below T_c; $\Delta G_a = \Delta G_m$ sensibly constant beyond T_c. Moreover the experimental variation of T_c with $\dot{\epsilon}$ can be written:

$$\dot{\epsilon}_1 = 3.5 \times 10^{-5}\text{ sec}^{-1} \rightarrow T_{c1} = 230 \pm 10\text{ K}$$

$$\dot{\epsilon}_2 = 2 \times 10^{-4}\text{ sec}^{-1} \rightarrow T_{c2} = 245 \pm 10\text{ K}$$

$$\dot{\epsilon}_3 = 7 \times 10^{-4}\text{ sec}^{-1} \rightarrow T_{c3} = 255 \pm 10\text{ K}$$

4. Discussion

As previously proposed [5], we confirm the existence of two distinct mechanisms responsible for yielding on both sides of a transition temperature T_c. At the lower temperatures a single mechanism is rate-controlling with a stress dependent free energy of activation; moreover the experimentally determined activation volume V_a indicates a strongly localized movement. This mode is clearly accounted for by a stress–temperature dependence of the strain rate in the form of Equation 1 and suggests a crystal-like plasticity through defect glide.

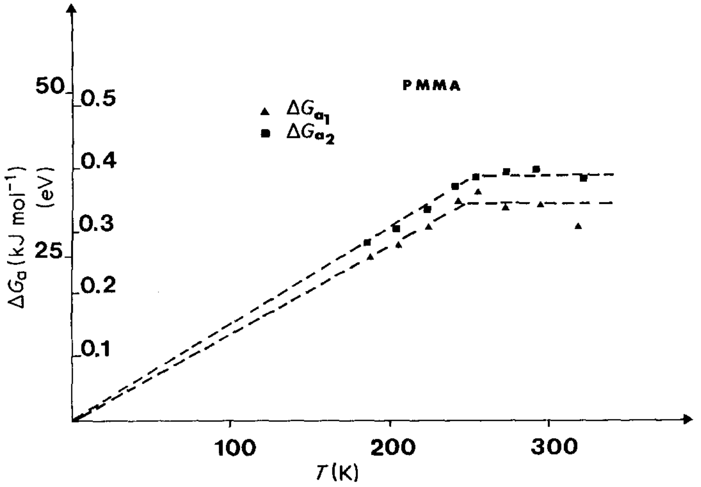

Figure 5 Variation of the Gibbs free energy of activation with temperature ($\dot{\epsilon} = 7 \times 10^{-4}$ sec^{-1}).

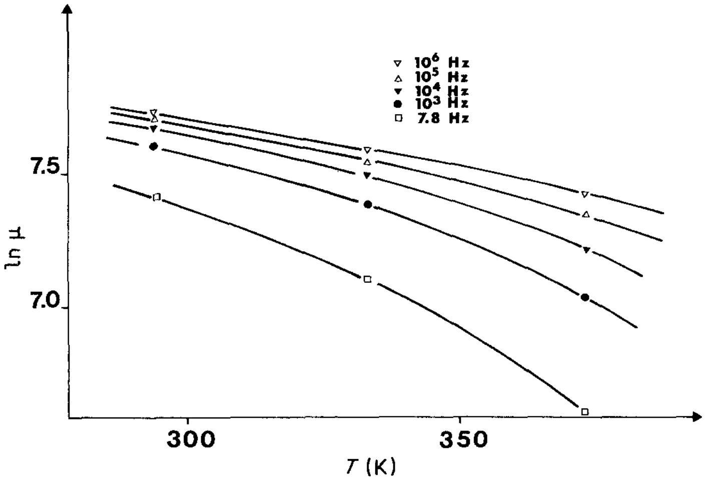

Figure 6 Variation of the shear modulus with temperature after Read [15] (logarithmic scale, μ in MPa).

On the other hand, the high temperature behaviour is characterized by a constant free energy of activation ΔG_m and by a stress dependence of the strain rate mainly limited to the pre-exponential term $\dot{\epsilon}_0$. A detailed analysis of the $\dot{\epsilon}_0$ dependences evoked in Section 2.3 with particular attention to the problem of internal stresses σ_i shall be given elsewhere.

Comparison with previously published data in the literature is not straightforward but should bring forth complementary information. The work of Bauwens-Crowet [13] provides us with a very complete set of data about compressive deformation of PMMA over a wide range of temperature and strain rate. As recalled in Section 2.2, a modified Ree–Eyring analysis is used to account for the observed stress–temperature behaviour: two independent processes are implied in the plastic deformation of PMMA – an α process involving large-scale movements of the chains typical of the glass transition, and a β process correlated to the first secondary relaxation evidenced by dynamical mechanical tests in this material.

Activation enthalpies are derived from a mathematical fitting of rheological equations to the data, and the existence of any entropy contribution is ignored in this way.

Nevertheless we have reconsidered these data from our own analysis despite the different origins of the materials [anionic PMMA (EAHP) as opposed to commercial Perspex (ICI)]. Transcription of data in the classical form $\sigma_y = f(T)$ is given in Fig. 7 where we show a reasonable agreement of shape with our curves (with a 10% difference in the magnitude of stresses at comparable temperature and strain rate). Derivation of activation parameters requires some assumptions. Due to the lack of experimental determination of V_0, we consider that the unique $V_0(\sigma)$ relationship exhibited in our measurements, shown in Fig. 8, is also valid for Bauwens-Crowet's data. In this way, we are able to express V_0, $\partial\sigma/\partial T$ and thus ΔH_0 for any stress and temperature level, from which we obtain an estimate of the free energy of activation against temperature for each considered strain rate.

The summary of Table II expresses the values obtained for three particular strain rates, together with the temperature shifts taken from Fig. 6 to account for the variation of shear modulus at the proper frequency. The results of Fig. 9 for the temperature variation of the free energy of activation depict the same kind of behaviour as found above in our data, with a range of constant value $\Delta G_m \simeq 0.4 \pm 0.04\,\text{eV}$.

Writing again the variation of T_c with $\dot{\epsilon}$ leads to

$$\dot{\epsilon}_1 \simeq 4 \times 10^{-5}\,\text{sec}^{-1} \rightarrow T_{c1} \simeq 240 \pm 10\,\text{K}$$

$$\dot{\epsilon}_2 \simeq 4 \times 10^{-3}\,\text{sec}^{-1} \rightarrow T_{c2} \simeq 270 \pm 10\,\text{K}$$

$$\dot{\epsilon}_3 \simeq 4 \times 10^{-1}\,\text{sec}^{-1} \rightarrow T_{c3} \simeq 300 \pm 10\,\text{K}$$

Note that the estimate of T_{c1} comes from an extrapolation of the $\sigma_y = f(T)$ curve at that particular strain rate since in the range experimentally investigated $\Delta G_a \sim \Delta G_m$ is sensibly a constant.

This whole set of data allows us to assess two final points. The first is a clear confirmation of the existence of two distinct deformation modes, a point recently confirmed on the molecular scale in deformed PS also, using the small angle neutron scattering technique [16].

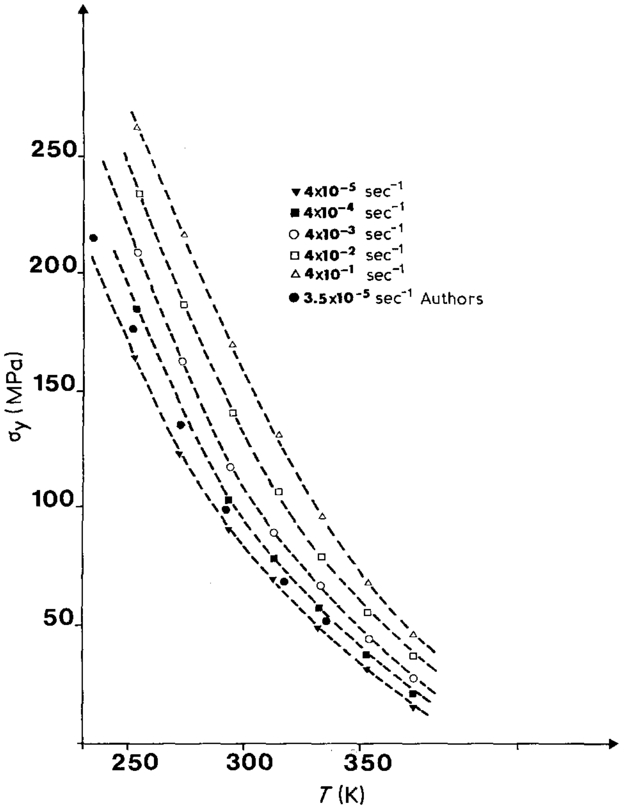

Figure 7 Variation of the yield stress with temperature after Bauwens-Crowet [13].

TABLE II Activation parameters (after Bauwens-Crowet [13])

T (K)	σ_a (MPa)	V_0 (nm^3)	ΔH_0 (kJ mol^{-1})	ΔG_a (kJ mol^{-1})	
$\dot{\epsilon}_p \sim 4 \times 10^{-5}$ sec^{-1}					
253	163	0.190	63.6	38.5	$\nu_{mod} = 1$ kHz
273	123	0.265	78	40.5	$\nu_{def} \lesssim 3$ kHz
295	91	0.380	86.7	37.6	
313	70	0.510	100.2	35.6	
333	50	0.760	136.8	39.5	
$\dot{\epsilon}_p \sim 4 \times 10^{-3}$ sec^{-1}					
183	379	0.110	28.9	25	$\nu_{mod} \sim 10^4$ Hz
203	321	0.115	33.7	27.9	(shift $\Delta T \sim 17$ K)
223	280	0.125	40.5	30.8	$\nu_{def} \sim 2 \times 10^4$ Hz
253	210	0.155	56.8	35.6	
273	162	0.205	72.2	39.5	
295	119	0.280	89.6	39.5	
313	91	0.380	101.1	41.4	
333	67	0.510	109.8	36.6	
353	44	0.880	154.1		
$\dot{\epsilon}_p \sim 4 \times 10^{-1}$ sec^{-1}					
253	262	0.125	41.4	30.8	$\nu_{mod} \sim 10^5$ Hz
273	216	0.150	54	34.7	(shift $\Delta T \sim 37$ K)
295	170	0.185	72.2	37.6	$\nu_{def} \sim 1.1 \times 10^5$ Hz
313	132	0.250	88.6	38.5	
333	97	0.350	102.1	39.5	
353	69	0.510	137.8		

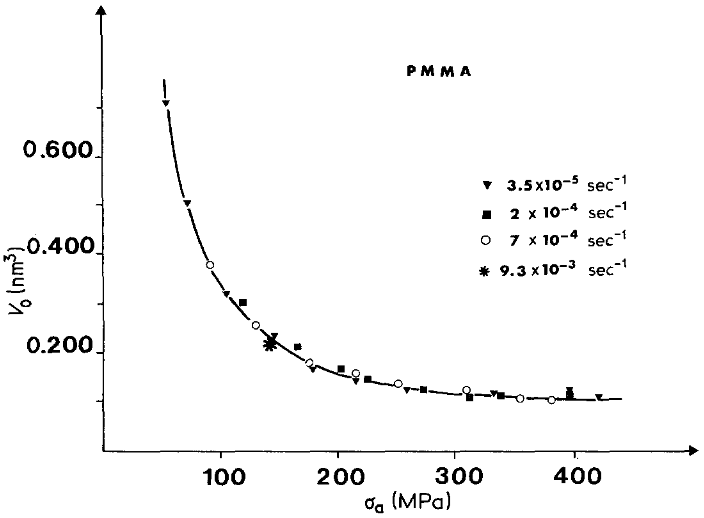

Figure 8 Stress dependence of the operational activation volume.

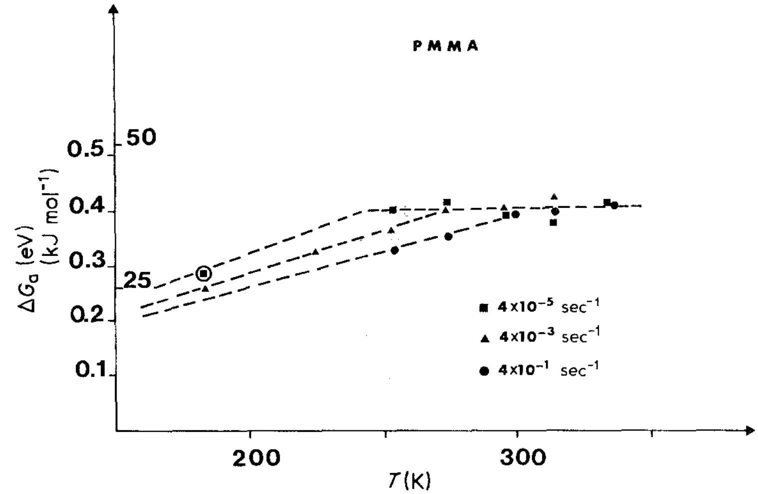

Figure 9 Variation of the Gibbs free energy of activation with temperature (from the data of Bauwens-Crowet [13]). The encircled square for $\dot{\epsilon} = 4 \times 10^{-5}$ sec^{-1} is deduced from an extrapolation of the yield stress–temperature data of Fig. 7.

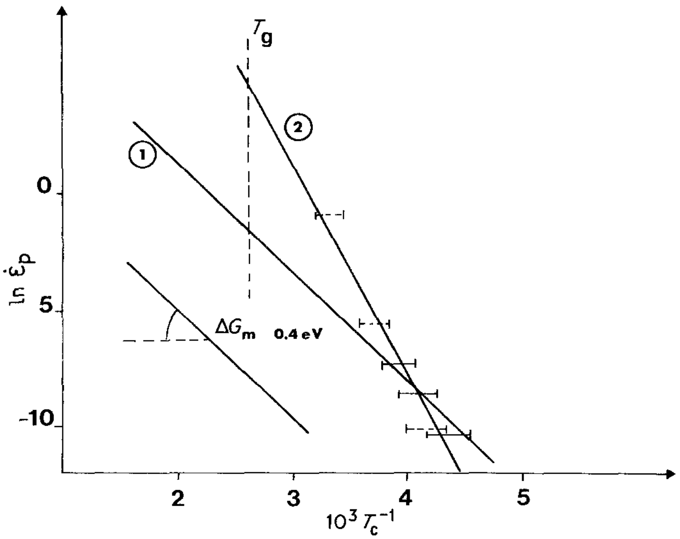

Figure 10 Variation of the logarithm of strain rate with the inverse of the transition temperature T_c. |——| our data, |- - - -| after Bauwens-Crowet [13]. 1, line with a slope proportional to ΔG_m; 2, best fit line for the whole data.

The second point is that T_c, the critical transition temperature from one mode to the other, increases clearly with $\dot{\epsilon}$. This is consistent with the rate equation written for $T = T_c$:

$$\dot{\epsilon} = \dot{\epsilon}_0 \exp - \left(\frac{\Delta G_m}{kT_c}\right)$$

Fig. 10 gives the experimental plot of $\ln \dot{\epsilon}$ against T_c^{-1}, the slope of which should be equal to $\Delta G_m \simeq 0.4$ eV provided that $\dot{\epsilon}_0$ remains constant. Although some accordance with this figure can be seen from our data, as given in Section 3.2, no such agreement can be claimed for the whole set of investigated values, which might mean that either some structural evolution or some adiabatic heating could affect the observed strain rate (i.e., $\dot{\epsilon}_0$), especially at high values.

Whatever it may be, it is of some interest to estimate the strain rate at which $T_c \simeq T_g$, which in practice means the minimum strain rate allowed in order to deform in the defect glide, chain orientation mode in the glass transition range. Fig. 10 roughly indicates, together with the above theoretical $\dot{\epsilon}(T_c)$ relationship, that figures like $\dot{\epsilon} \sim 10^0$ to 10^2 sec^{-1} are predicted, which are obviously below the usual processing values. This result shows that usual processing conditions deal probably with our *low* temperature deformation mode.

To conclude, on the basis of this clearly identified plastic deformation behaviour, the question of the relationship of parameters like ΔG_m and T_c to specific molecular features of the material is now raised. We shall report on this problem in a forthcoming paper.

References

1. P. B. BOWDEN and S. RAHA, *Phil. Mag.* **22** (1970) 463.
2. J. C. B. WU and J. C. M. LI, *J. Mater. Sci.* **11** (1976) 434.
3. B. ESCAIG and J. M. LEFEBVRE, *Rev. de Phys. Appliquée* **13** (1978) 285.
4. J. P. CAVROT, J. HAUSSY, J. M. LEFEBVRE and B. ESCAIG, *Mater. Sci. Eng.* **36** (1978) 95.
5. J. HAUSSY, J. P. CAVROT, B. ESCAIG and J. M. LEFEBVRE, *J. Polym. Sci. Polym. Phys. Ed.* **18** (1980) 311.
6. J. M. LEFEBVRE, Thèse de Doctorat d'Etat ès Sciences Physiques (1981).
7. B. ESCAIG, in "Plastic Deformation of Amorphous and Semi-crystalline Materials", edited by B. Escaig and C. G'Sell (Les Editions de Physique, Les Ulis, 1982) p. 187.
8. P. B. BOWDEN and S. RAHA, *Phil. Mag.* **29** (1974) 149.
9. M. CAGNON, *ibid.* **24** (1971) 1465.
10. U. F. KOCKS, A. S. ARGON and M. F. ASHBY, "Process in Materials Science 19", (Pergamon Press, Oxford, 1975) p. 110.
11. A. S. ARGON, *ibid.* **28** (1973) 839.
12. J. C. BAUWENS, *J. Mater. Sci.* 7 (1972) 577.
13. C. BAUWENS-CROWET, *ibid.* 8 (1973) 968.
14. C. BULTEL, J. M. LEFEBVRE and B. ESCAIG, *Polymer* **24** (1983) 476.
15. B. E. READ, *ibid.* **22** (1981) 1580.
16. J. M. LEFEBVRE, C. PICOT and B. ESCAIG, *ibid.* **23** (1982) 1751.

Received 1 November 1983
and accepted 13 March 1984